



Estimating salinity to complement observed temperature: 2. Northwestern Atlantic

W.C. Thacker^{a,*}, L. Sindlinger^b

^a *Atlantic Oceanographic and Meteorological Laboratory, 4301 Rickenbacker Causeway, Miami FL 33149 USA*

^b *Rosenstiel School of Marine and Atmospheric Science, 4600 Rickenbacker Causeway, Miami FL 33149 USA*

Received 23 September 2004; accepted 14 June 2005

Abstract

This paper addresses the problem of estimating salinity for a large region in the Atlantic Ocean containing the Gulf Stream and its recirculation. Together with Part 1 [Thacker, W.C., 2006-this issue. Estimating salinity to complement observed temperature: 1. Gulf of Mexico. *Journal of Marine Systems*. doi:10.1016/j.jmarsys.2005.06.008.] dealing with the Gulf of Mexico, this reports on the first efforts of a project for developing world-wide capability for estimating salinity to complement expendable-bathymograph (XBT) data. Such estimates are particularly important for this region, where the strong frontal contrasts render the task of assimilating XBT data into numerical models more sensitive to the treatment of salinity.

Differences in salinity's co-variability with temperature and with longitude, latitude, and day-of-year from the northwestern part of the region with the Gulf Stream to the southeastern part more characteristic of the Sargasso sea suggested that the region be partitioned to achieve more accurate salinity estimates. In general, accuracies were better in the southeastern sub-region than in the more highly variable northwestern sub-region with root-mean-square estimation errors of 0.15 psu at 25 dbar and 0.02 psu at 300 dbar as compared with 0.35 psu and 0.50 psu, respectively, but in the southeast there was an unexpected error maximum around 1000 dbar where estimates were slightly less accurate than in the northwest. For pressures greater than 1400 dbar root-mean-square errors in both sub-regions were less than 0.02 psu.

© 2006 Elsevier B.V. All rights reserved.

Keywords: XBT; CTD; Regression; Data assimilation; HYCOM

1. Introduction

The companion paper (Thacker, 2006-this issue) introduces a project for developing the capability of estimating salinity from observations of temperature, so that salinity can be corrected when expendable-bathymograph (XBT) data are assimilated into numerical models of oceanic circulation. The success reported there for estimating salinity for the Gulf of Mexico with

its Loop Current suggested that the next step should be to investigate a large, highly variable region in the North Atlantic Ocean containing the Gulf Stream. Similar success for this region would indicate that relatively large and complicated regions might be addressed without having to deal with more, smaller regions that would slow the progress of the project.

As the project is still in an exploratory stage, the exact boundaries of the region to study were quite arbitrary, so the 30° longitude by 20° latitude region for this study shown on the map in Fig. 1 was chosen with the thought that experience here might provide guidance for the

* Corresponding author.

E-mail address: carlisle.thacker@noaa.gov (W.C. Thacker).

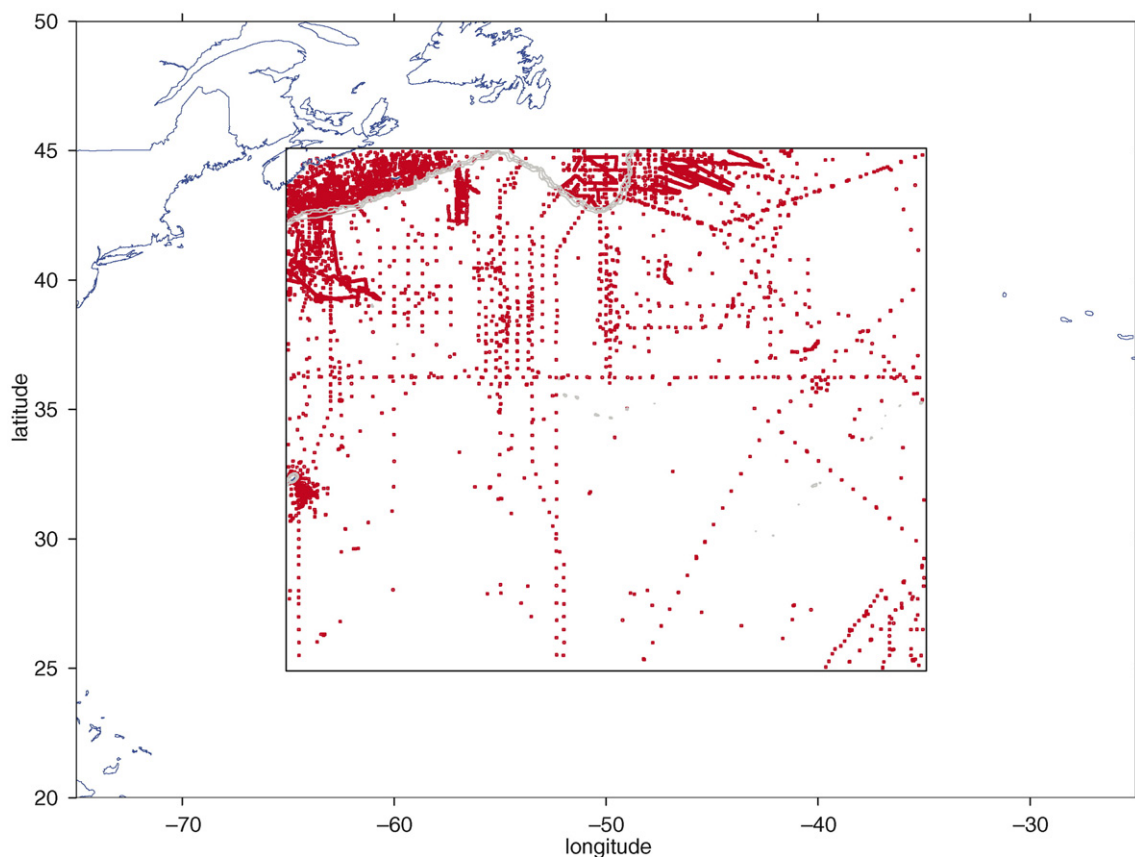


Fig. 1. Map of the North Atlantic Ocean showing the area addressed in this study. Red dots represent the 11,644 CTD stations from the World Ocean Database 2001 for the rectangular region. Bathymetric contours at 500, 1000, 1200, and 2000 m are indicated in gray.

choice of other regions as the study progresses. Nova Scotia can be seen at its northwest corner, the Bahamas to the southwest, and the Azores to the east; Bermuda is on its western boundary. Except for the Scotian Shelf and the Grand Banks, most of the region is very deep.¹ Both temperature and salinity exhibit a wide range of variability across this large region. In particular, they change abruptly across the fronts associated with the meandering Gulf Stream (Watts, 1983) and with the drifting warm-core eddies to its north and cold-core eddies to its south (Richardson, 1983). Moreover, the region is open with nothing preventing water from crossing its arbitrary boundaries. While the primary external influence is that of the Gulf Stream entering from the west, water from the Labrador Current impinges from the north (Loder et al., 1998), and there are less pronounced exchanges across the southern and eastern boundaries.

In spite of this region's size and complexity and the wide ranges over which its salinity and temperature vary, throughout the region salinity exhibits a pronounced co-variability with temperature. Scatter plots of temperature vs. salinity at fixed pressure show data throughout the region cluster along relatively well-defined curves.² While this co-variability is relatively weak near the ocean's surface, it is stronger in and below the thermocline, allowing knowledge of temperature to restrict the range of salinity by more than an order of magnitude. Still, the various water types encountered in this region contribute to the spread of salinity values. If they could be identified and treated separately, accuracy might be improved. Unfortunately, identifying the water type from temperature and location is difficult and deserves a separate study. The challenges of the continental shelf are finessed by basing the salinity

¹ Thanks are extended to Dong-Shan Ko of the Naval Research Laboratory for providing the DBDB2 bathymetric data. The contours in Fig. 1 are not labelled, but the shelf can be identified from the closely spaced contours in the north.

² To study water-mass anomalies Armi and Bray (1982) describe the TS curve over a wide pressure range using a cubic-spline function. Their fit was not to the measurements but to curves from two previous analyses (Iselin, 1936; Worthington and Metcalf, 1961).

estimates on data from the deeper parts of this rather arbitrary rectangle. Still, some of these data reflect intrusions of the colder, fresher water from the shelf. Furthermore, some of the spread appears to be associated with a difference between the northwestern part of the region, which is the domain of the Gulf Stream and its recirculation, and the southeastern part, which might be regarded as part of the Sargasso Sea. Just as the choice of the rectangle was arbitrary, so is the position of the boundary between northwest and southeast sub-regions. Even though this study is primarily exploratory, with the intent to discover the problems that must be overcome, and even though the results might be improved with additional effort, the empirical relationships presented here for estimating salinity in this region are extremely useful.

In the northwestern sub-region, for pressures greater than 300 dbar, i.e., in and below the thermocline, the tight relationship between temperature and salinity allows a fourth-degree polynomial of temperature to estimate salinity with root-mean-square (rms) errors smaller than 0.05 psu. Nearer the surface, where the TS relationship is less well-defined, no empirical function of temperature can provide such accurate estimates of salinity. However, using longitude and day-of-year as supplemental regressors can compensate to some extent, reducing errors at 25 dbar from the temperature-only level of roughly 0.6 psu to approximately 0.43 psu. As surface salinity might soon become routinely observed from space, it is interesting to note that it might allow rms errors for estimates of salinity at 25 dbar to be reduced to 0.3 psu.

In the southeastern sub-region, different models were needed. A second-degree polynomial of temperature was sufficient to capture TS co-variability, and both longitude and latitude provided useful information about salinity, even at depth, as did day-of-year. While overall the accuracies for estimating salinity in this sub-region were higher than for the northwest with rms errors below 0.025 psu between 250 dbar and 700 dbar and only 0.15 psu at 25 dbar, there was a local rms-error maximum of 0.07 psu in the vicinity of 1000 dbar.

2. CTD data

The locations of the 11,644 CTD stations from the National Oceanographic Data Center's World Ocean Database 2001 (Conkright et al., 2002b), which might be used to establish empirical relationships between salinity and temperature for the region from 65°W to 35°W and from 25°N to 45°N, are shown as dots on the map in Fig. 1. These stations were occupied during years 1970 to 2000 with the bulk of the data collected in summer months; there were only 1398 for months

November through March but 10246 for April through October. Over half (6782) of these stations are in water where the bottom depth is less than 1000 m, which is so well sampled that dots for some stations obscure others, while the deeper regions are less well sampled. The sampling is far from uniform; some areas are essentially over sampled while others are hardly sampled at all. In particular, there are far fewer stations in the southern half of the region than in the northern half and fewer in the east than in the west. Still, there are parts of the world, especially in the southern hemisphere with much less data, so this region should be considered to be data-rich. In fact there are far more data than are needed, and working with so many profiles is inconvenient.

Because the continental shelf offers its own complications for estimating salinity, we decided to focus on the deeper water. While many of the profiles in the deeper regions fail to descend below the range of XBTs, enough do to allow empirical relationships between salinity and temperature to be established using data from the same profiles at all depths. After excluding those profiles that do not reach 1600 dbar,³ those that start deeper than 25 dbar, and those that have gaps greater than 10 dbar, the remainder were interpolated linearly to standard pressure levels at 25 dbar intervals. Then the few profiles with extreme outliers⁴ and with potential-density inversions greater than 0.03 kg/m³ were discarded,⁵ leaving 1390 profiles with which to work. Fig. 2 shows the locations of these 1390 stations.

Before proceeding with the task of identifying empirical models from these CTD data, it is useful to explore how they are distributed. Fig. 3 uses box-and-whisker plots to summarise the distributions of temperature and salinity from the 1390 profiles at standard pressure levels. The central dots in these plots indicate the medians of the data at each pressure level; the boxes indicate the inter-quartile ranges containing the values for half the data for that level, the whiskers extend from each end of the box to the nearest value within 1.5 times the box's width to indicate the expected range of the data; and the more extreme values are indicated with dots. A few data can be seen as isolated outliers, which

³ The deepest level considered by Thacker (2006-this issue) is 1600 dbar. In that study, there were far fewer long profiles, so profiles with differing lengths were used.

⁴ Temperatures were required to be between 0 °C and 30 °C, salinities were required to be between 25 psu and 38 psu, and potential densities relative to the surface were required to be greater than 1022 kg/m³.

⁵ Whereas a smaller value was used in part 1 for the Gulf of Mexico (Thacker, 2006-this issue), 0.03 kg/m³ is roughly the accuracy to which potential density can be estimated by the equation of state (Tomczak and Godfrey, 2003; Millero and Poisson, 1981).

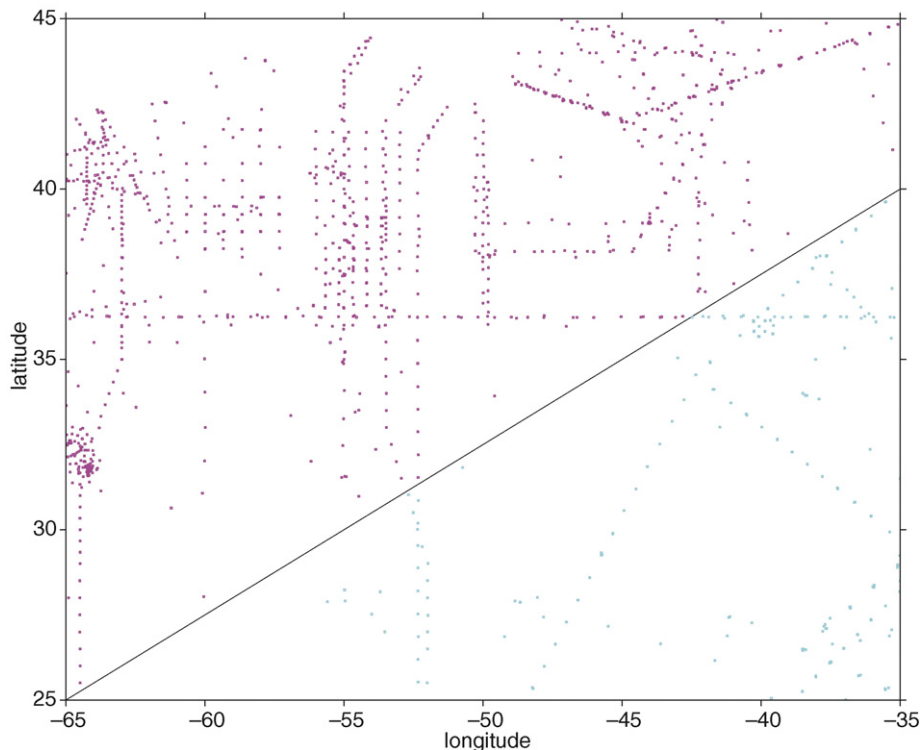


Fig. 2. Locations of the 1390 stations with long profiles. Colors correspond to those used in Fig. 5.

could indicate either bad data or unusual natural variability, but any bad data that might have values within the ranges of the whiskers are not revealed.

Unlike box-and-whisker plots for the Gulf of Mexico (Thacker, 2006-this issue), which allowed the identification of bad data as detached outliers, these show very few outliers, detached or otherwise, most of which are cold and fresh and above 400 m and appear to be consistent with water that has intruded from the shelf. While fewer outliers might be taken as an indication that these data are much cleaner than those for the Gulf, and they are in fact cleaner, the differences regarding outliers stems from differences in the sizes of the inter-quartile ranges: about 10 °C and 1.25 psu for pressures less than 500 dbar for these data as compared to less than 2 °C and 0.4 psu for the Gulf data. The smaller inter-quartile ranges for the Gulf data lead to shorter whiskers and allow more outliers, while the larger ranges for these data cause the whiskers to extend to encompass most of the data.

The histograms in Fig. 4 show in more detail how the values of temperature and salinity for the 1390 profiles are distributed at 400 dbar. The inter-quartile ranges in Fig. 3 are large, because the distributions are multimodal. The shapes of the histograms do not necessarily indicate the frequency with which water having these properties might be encountered, as the sampling

reflects oceanographers' preferences for studying interesting features. Such bias is difficult to avoid, and complicates the task of estimating climatological means of temperature and salinity. Fortunately, the impact of sampling bias on estimates of salinity from temperature should be relatively minor, as such estimates are based on curves fitted to scatter plots of temperature vs. salinity, and sampling bias manifests as increased data for some portions of the TS curve.

Fig. 5 shows such scatter plots for the data at four pressure levels. The peaks in the histograms of Fig. 4 appear here in the scatter plot for 400 dbar as local increases in the density of points. These variations in density do not detract from the fact that the points fall into a long thin cluster that can be well described by a smooth curve. Note that there are a few isolated points, which would be the most distant from the curve; only those that are at the extremes of the ranges of temperature or salinity would be flagged by box-and-whisker plots or by histograms as possibly bad data.

In these scatter plots colors are used to indicate whether the data are from the northwest (magenta) or southeast (cyan) sub-regions that are indicated in Fig. 2. The ranges of variability of temperature and salinity are less in the southeast away from the Gulf Stream front. While the data from both regions appear to have the same

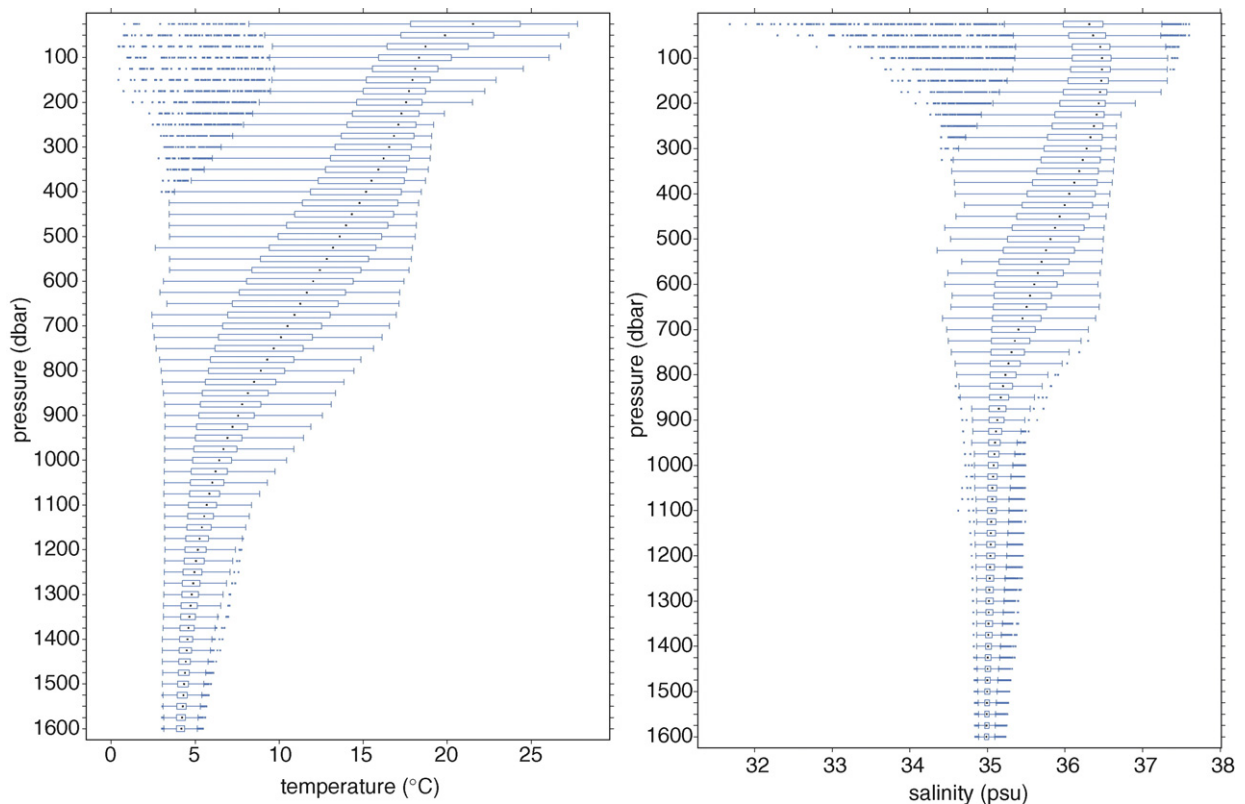


Fig. 3. Box-and-whisker plots of temperature (left) and salinity (right) for data from the 1390 stations of Fig. 2 interpolated to standard pressure levels at 25 dbar intervals.

TS relationship at 400 dbar, this is not the case for the other levels. At 100 dbar the secondary cluster of warm-salty data is seen to come from the southeast region. While the cyan points for warmer and saltier values merge with magenta points, they do suggest that at 100 dbar the TS relationship for the southeastern data differs from that for the northwestern data. At 800 dbar and 1200 dbar the southeastern water is again seen to be more salty than the northwestern. Similar plots for the other levels, which are not shown, indicate a gradual transition from a near-surface behaviour similar to what is shown for 100 dbar, to a thermocline behaviour like that for 400 dbar, to a fresher bulge like for 800 dbar, to separation of warm-salty from cold-fresh like 1200 dbar. The division between northwest and southeast was quite arbitrary; a different partition might correspond to a better separation of clusters at some levels and worse at others. Nevertheless, it is clear that the relationship between salinity and temperature is not homogeneous over the entire region.

The CTD data for the stations indicated in Fig. 2 were divided into two groups, one for the northwestern sub-region and the other for the southeastern sub-

region. As the latter is likely to belong to a larger Sargasso Sea region and our primary focus is on the Gulf Stream front, most of our attention will be devoted to the northwestern part. To avoid redundant information, stations within each sub-region were thinned; they were ordered by date, time, then by latitude, and then by longitude as in Part I (Thacker, 2006-this issue), and all stations were discarded that were within 0.3 degrees latitude or longitude or within 2 days of the previous in the sequence, retaining the first of each sub-sequence of close stations without making an effort to choose the best within the subsequence. The remaining data in each sub-region were randomly partitioned⁶ (Fig. 6) with one half to be used for fitting regression models and the other, for gauging performance.

3. Northwestern sub-region

The S-shape of the distributions of the northwestern data in the TS plots of Fig. 5 suggest that salinity might

⁶ The random partition was made using the R software function sample (R Development Core Team, 2004; Venables and Ripley, 2002).

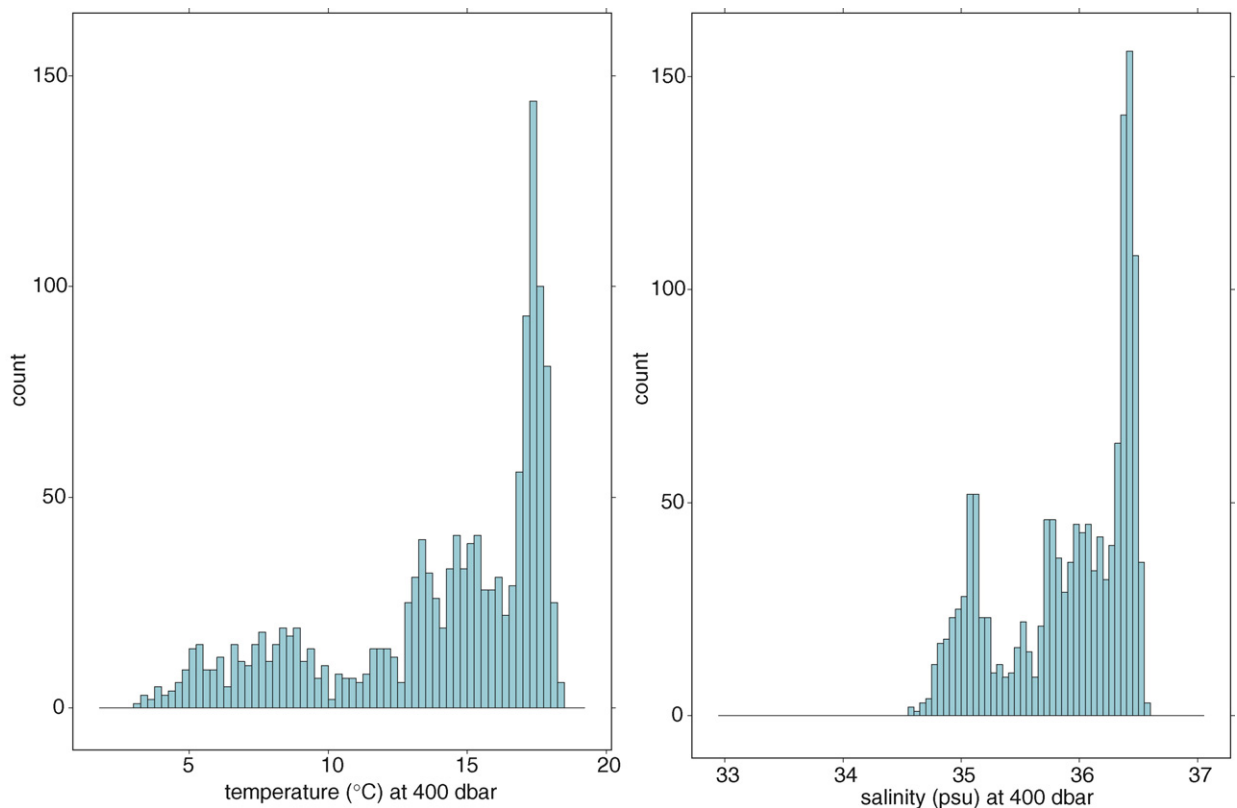


Fig. 4. Histograms of temperature (left) and salinity (right) for data at 400 dbar. Bin widths are 0.25 °C for temperature and 0.05 psu for salinity.

be modelled by polynomials of temperature of 3rd or higher degree, and that proved to be the case. Polynomials of temperature 4th degree and less were fitted to the training data at each pressure level. For example, in fitting the 4th-degree polynomial,

$$\hat{S} = P_4(T) = a_0 + a_1 T + a_2 T^2 + a_3 T^3 + a_4 T^4, \quad (1)$$

the coefficients⁷ $a_0(p)$, ..., $a_4(p)$ were adjusted to give the best possible robust agreement with the training data.⁸

Two empirical models, which are not regression models, were also considered. The first estimates the salinity at each pressure level by the climatological mean salinity at that level,

$$\hat{S} = \langle S \rangle_p, \quad (2)$$

⁷ For notational simplicity the same symbol is used for the coefficient at the different pressure levels and for polynomials of different degrees. The value of a_0 , for example, is different at each pressure level and changes with the degree of the polynomial.

⁸ Computations were made using the R software (R Development Core Team, 2004) function `rlm` for robust least-squares regression with the M-estimation method (Venables and Ripley, 2002).

where $\langle \rangle_p$ indicates the mean for fixed pressure. In this case the mean has been computed from the training data, but it could have been derived from published climatologies (Conkright et al., 2002a), circumventing the need to work with the CTD data.⁹ The second estimates salinity by its climatological mean on temperature surfaces:

$$\hat{S} = \langle S \rangle_T, \quad (3)$$

a method that dates back to Stommel (1947). The training data were interpolated to standard temperatures at 0.1 °C intervals to compute the means, and then the means were interpolated to get estimates of salinity at the standard pressure levels. This method can also be implemented, at least approximately, without the effort of working with the CTD data by using the mean temperature and salinity profiles to approximate $\langle S \rangle_T$.

Fig. 7 shows the root-mean-square errors when these models are used to estimate the independent verification data. Errors for estimates based on the climatological

⁹ Thacker et al. (2004) have discussed the disadvantages of using this method within the context of assimilating XBT data into numerical models of oceanic circulation.

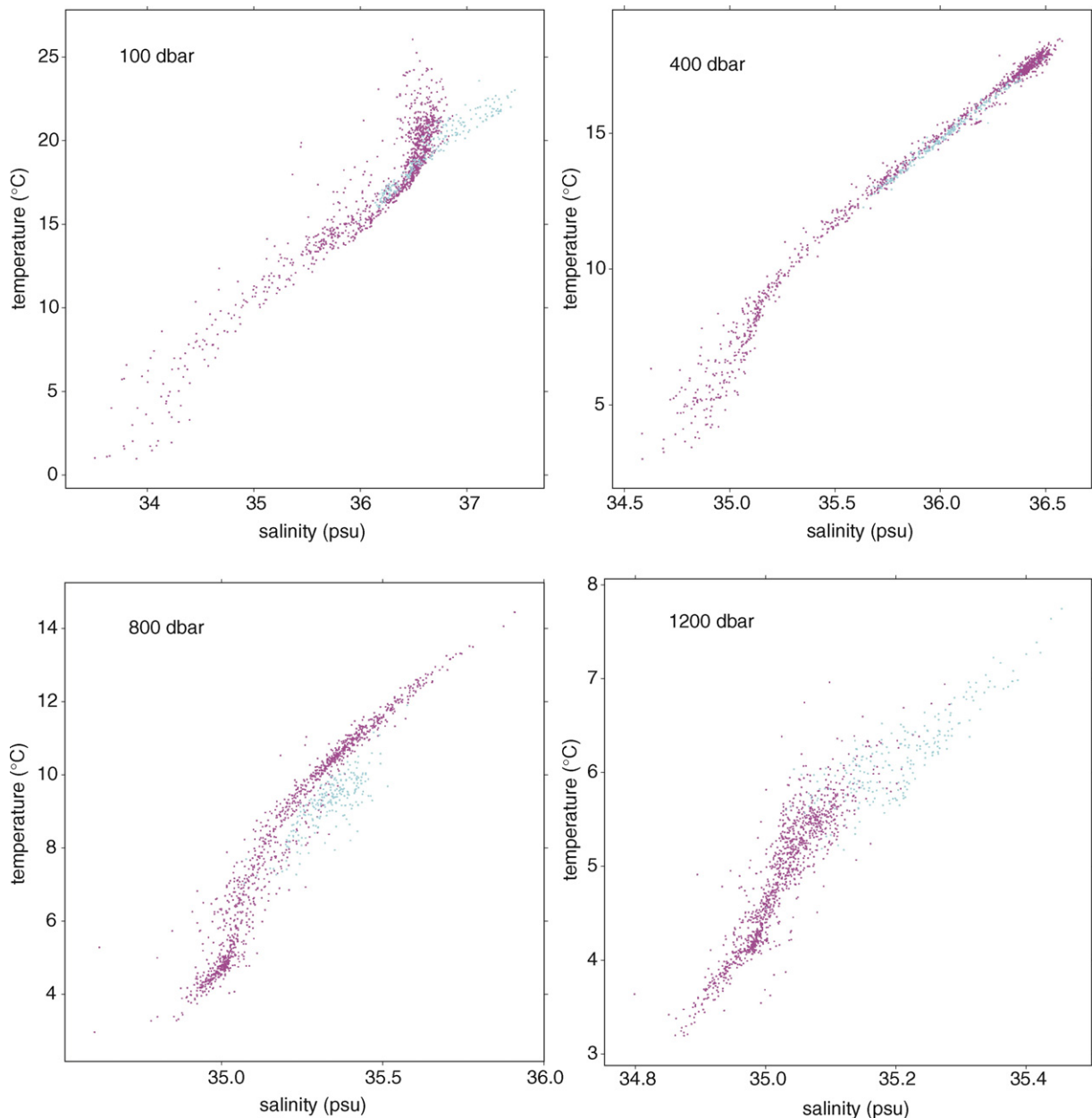


Fig. 5. Scatter plots at four pressure levels with colors indicating region.

mean salinity on pressure surfaces were so large that it is not competitive at any pressure level. The climatological mean on temperature surfaces provides more accurate estimates,¹⁰ but those errors are roughly twice as large as for the 4th-degree polynomials of temperature. Errors

¹⁰ For the warmest observed temperatures, only a small number of training profiles contribute to the estimation of average salinity and, similarly, near the surface not all verification profiles contribute to the computation of rms errors.

for lower-degree polynomials¹¹ were also smaller than those for Stommel's method. If plotted at the same scales used in Fig. 7 no differences between the rms verification errors for 3rd-degree and 4th-degree polynomials could be seen, even though those for the 4th-degree polynomials are a bit smaller. Errors for the 2nd-degree polynomials are noticeably larger between 75 dbar and 375 dbar than those for polynomials of

¹¹ Those curves were omitted from Fig. 7 to make it easier to read.

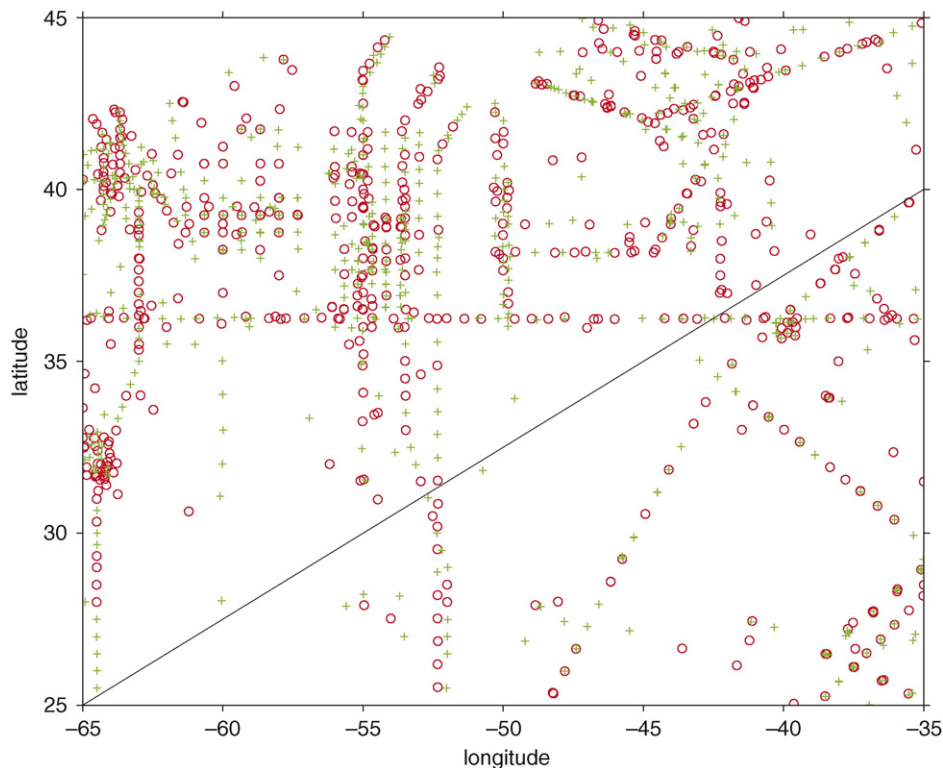


Fig. 6. Locations of stations contributing training data o (467 in NW, 114 in SE) and verification data + (468 in NW, 114 in SE).

3rd and 4th degree, but still substantially smaller than those for Stommel's method. Even the straight line (1st-degree polynomial) performs better substantially than Stommel's method everywhere except between 500 dbar and 725 dbar, and it performs as well as the other polynomial models for pressures greater than 900 dbar.

Fig. 8 shows the verification data at 200 dbar overlaid with the estimates from the three models. Horizontal distances from the points to each curve is the error for that point using that model. The vertical red line, which is the temperature-independent estimate based on the mean salinity at 200 dbar, totally ignores the strong TS co-variability and thus has a large rms error. The green curve representing the pressure-independent estimate based on the mean salinity on temperature surfaces does much better at representing the co-variability, so its errors are smaller; still, it is systematically too fresh for temperatures above 13 °C and too salty below 11 °C. The 4th-degree polynomial of temperature, on the other hand, lies near the center of the data at all temperatures¹² and consequently has the

smallest rms error. If the curve for the 3rd-degree polynomial of temperature were added, it too would provide an excellent approximation of the data; it would be very nearly the same as the blue curve over much of the temperature range, with noticeable differences only at the extremes. Similarly, if curves for 1st- and 2nd-degree polynomials were added, while not as good an approximation to the data as those of 3rd- and 4th-degree, they would nevertheless be considerably better than the green curve.

For pressures greater than 300 dbar temperature alone provides sufficient information to estimate salinity to an accuracy of 0.05 psu, but the rms errors increase to more than 0.6 psu at 25 dbar. When residuals of the near-surface $P_4(T)$ models were plotted vs. the day of the year and vs. longitude, some systematic behaviour was observed, suggesting that seasonal or locational effects might be exploited to improve the accuracy of near-surface salinity estimates. However, there appeared to be little systematic variation with latitude.

Fig. 9 shows that the residuals for the robustly fitted 4th-degree polynomial model for 25 dbar do not vary uniformly across the seasonal cycle. Moreover, their behaviour is not sinusoidal. Instead, the model underestimates more and more data as the year progresses through October

¹² The blue curve is *not* the best-fit to these data but to the training data.

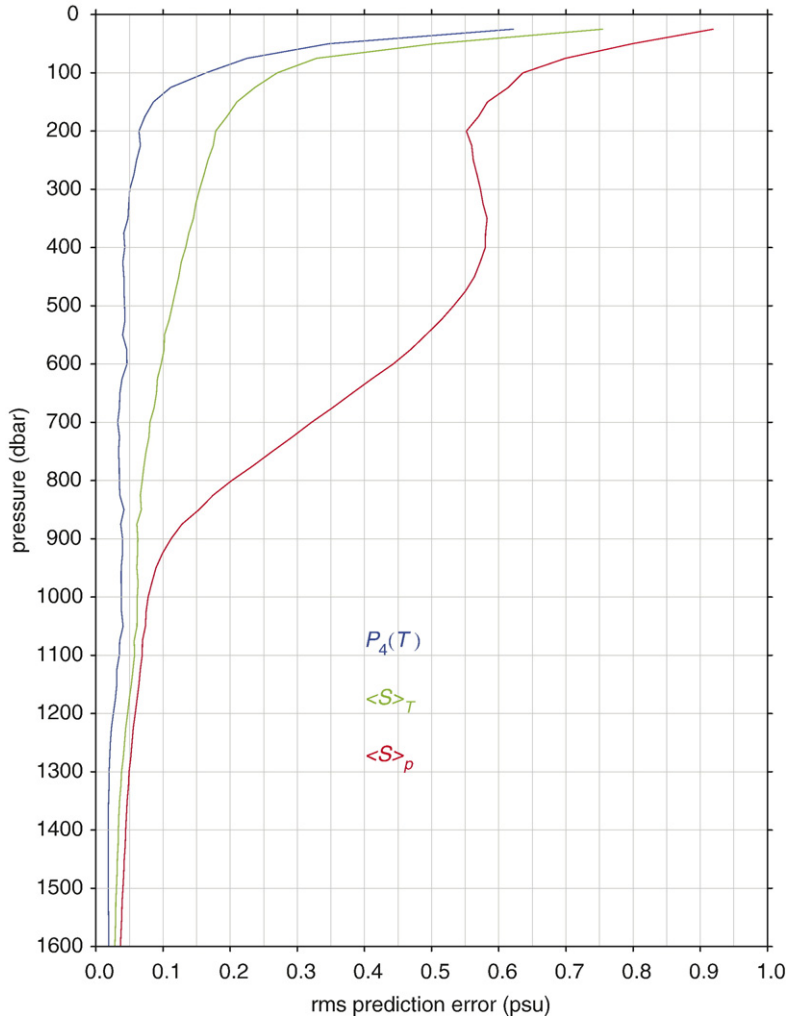


Fig. 7. Root-mean-square differences between verification data from the northwestern sub-region and their estimated counterparts. Blue curve corresponds to 4th-degree polynomials of temperature. Green and red curves correspond to means of training salinity on temperature and pressure surfaces, respectively.

followed by a rapid transition at the end of the year, with both mean and standard deviation varying as a function of day-of-year d . While supplementing $P_4(T)$ with a polynomial function of d does not address the heteroscedasticity directly, it should improve the estimates of near-surface salinity. The lack of long profiles during the winter months further complicates matters, and a better treatment would involve the use of some of the shorter profiles. Nevertheless, it is interesting to see what these data reveal.

The residuals of the $P_4(T)$ model also exhibited systematic near-surface behaviour when plotted vs. longitude λ and vs. surface salinity S_0 . Consequently a variety of other models were examined. Here, we report the results of three of these:

$$\hat{S} = P_4(T) + \tilde{P}_4(d) = a_0 + a_1T + a_2T^2 + a_3T^3 + a_4T^4 + b_1d + b_2d^2 + b_3d^3 + b_4d^4, \quad (4)$$

which adds to (1) terms proportional to the first four powers of the day of the year,¹³

$$\hat{S} = P_4(T) + \tilde{P}_4(d) + \tilde{P}_1(\lambda), \quad (5)$$

which adds to (4) a term proportional to the longitude of the station, and

$$\hat{S} = P_4(T) + \tilde{P}_4(d) + \tilde{P}_1(\lambda) + \tilde{P}_1(S_0), \quad (6)$$

which adds to (5) a term proportional to the surface salinity.

While the training and verification data used for the models of Fig. 7 could be used for models (4) and (5) involving d and λ , only the subset of profiles measuring

¹³ The tilde is used to indicate that the constant term is absent from $\tilde{P}_4(d)$ as only one constant term is needed.

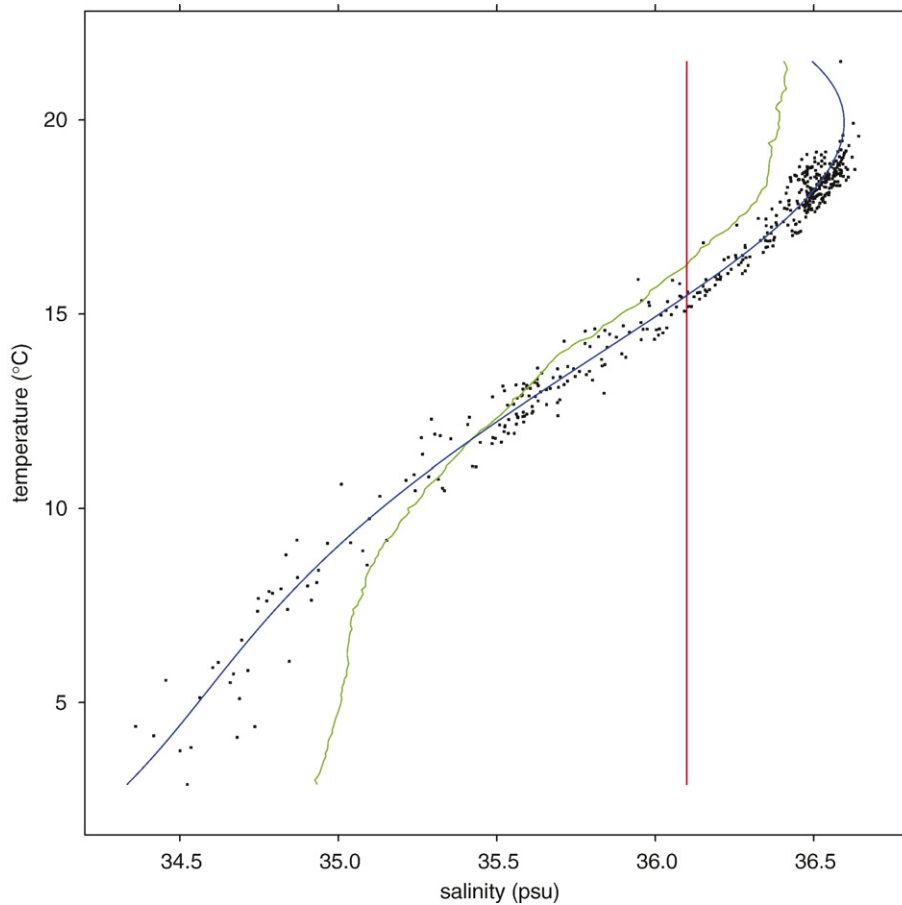


Fig. 8. Points represent verification data from northwestern sub-region at 200 dbar and the curves represent estimates based on the training data for the same region: blue curve, 4th-degree polynomials of temperature; green curve, climatological mean salinity on temperature surfaces; vertical red line, mean salinity at 200 dbar.

salinity close to the surface can be used for model (6). In order to judge fairly how much impact satellite-based measurements of sea-surface salinity might have beyond what is provided by d and λ , all of these models were fitted to and scored against profiles providing data for pressures less than or equal to 2 dbar, using the data nearest the surface as proxies for satellite-based observations of surface salinity.¹⁴ Fig. 10 shows the rms errors for these models together with those for the 4th-degree polynomial of temperature, which have been recomputed using this subset of profiles.¹⁵ Only errors for the upper 300 dbar are shown, as these models all had essentially the same rms errors below this level. The day

of the year d clearly provides additional information for pressures less than 100 dbar. Linear, quadratic, and cubic dependence on d gave increasingly better results with those for the 3rd-degree polynomials performing almost as well as 4th-degree, modelling seasonal effects with sinusoids was not successful. Longitude provides additional information about the near-surface salinity beyond what is contributed by temperature and day-of-year. Including a term proportional to longitude reduced the rms error at 25 dbar to 0.35 psu, but quadratic or higher function of longitude offered no further improvement. Unlike longitude, latitude did not prove to be useful in this sub-region.

It is interesting to note the effect of the different samples on the rms errors of model (1). Fig. 7 indicates the rms error at 25 dbar to be 0.62 psu when coefficients are determined from the full set of training profiles and predictions are scored against the full set of verification profiles, while Fig. 10 indicates the smaller value of

¹⁴ These models were fitted to 176 training profiles and verified with 194 profiles.

¹⁵ The results for the models not involving surface salinity, when fitted to the full training set and scored for the full verification set, were similar.

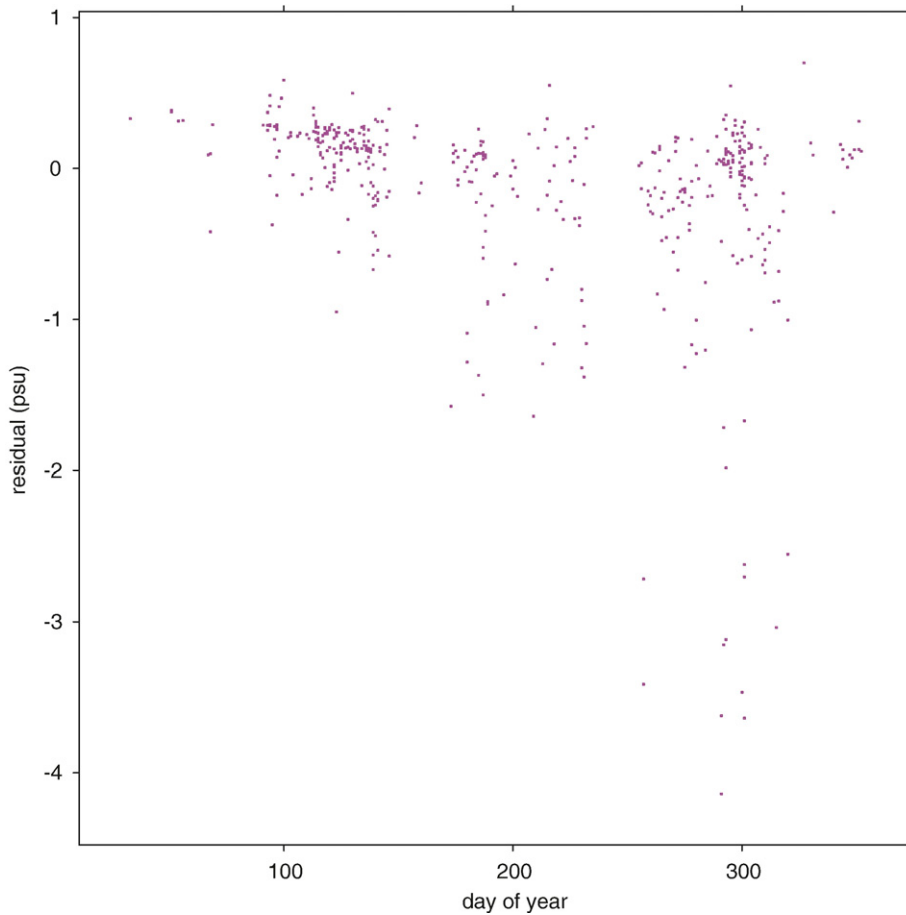


Fig. 9. Residuals for the robustly fitted 4th-degree polynomial of temperature at 25 dbar for the northwestern sub-region vs. day-of-year.

0.57 psu when the subsets of profiles that provide surface measurements are used. Similarly, the errors at 50 dbar, in the same order, are 0.35 psu and 0.30 psu. Such large changes are confined to the upper 100 m, all corresponding to smaller errors when using fewer profiles. On the other hand, for pressures greater than 200 dbar the errors for the subset are generally larger than those for the full set by about 0.01 psu. The rms fractional difference between the two error profiles over the 64 pressure levels of 0.11% might be taken as a measure of the accuracy of the error estimates.

Fig. 11 compares 28 randomly selected¹⁶ verification profiles from the northwestern sub-region with their counterparts estimated using longitude and the first four powers of temperature and of day-of-year as predictors (Eq. (5)) with its nine coefficients determined by fitting to the full set of 466 training profiles. As surface salinity is not available for most of the archived XBT data, this is the

best model considered here. While there are some large differences near the surface, the agreement is quite remarkable overall. The principal problem below the surface is the failure to capture the strength of the fresh intrusions seen for profiles 3280759 and 3345297. The systematic offset for profile 3364059 over its entire length suggests that the salinity measurements for this profile might not have been properly calibrated. While a motivation for these estimates, beyond providing a basis for correcting salinity when assimilating XBT data into numerical models, was their use for checking the calibration of salinity profiles in the CTD archives in a manner similar to that used by Wong et al. (2003) for profiling floats, another application might be checking for possibly miscalibrated salinity profiles in the CTD archives.

Fig. 12 shows the accuracy of potential density based on salinity estimated using the same model (Eq. (5)) as used for the profiles in Fig. 11. The equation of state of sea water (Fofonoff, 1977) was used at each pressure level to compute potential density first from observed temperature

¹⁶ The random selection was made using the R function sample.

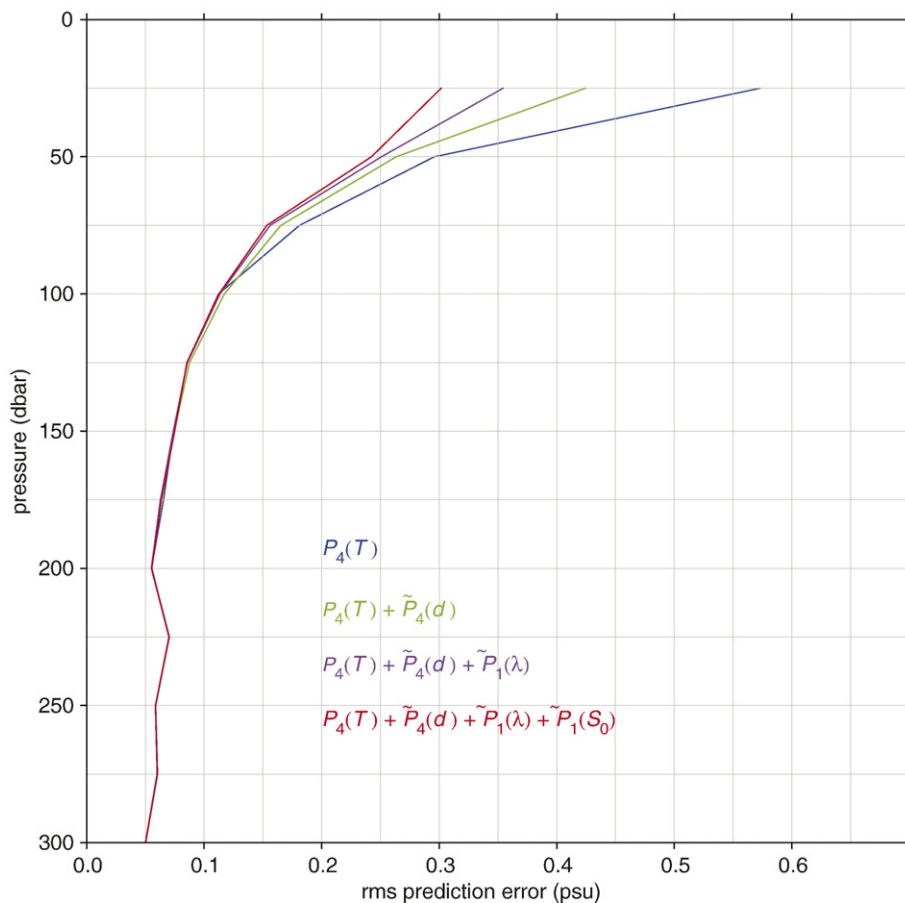


Fig. 10. Root-mean-square errors for salinity models for the northwestern sub-region with increasing numbers of regressors. The blue curve corresponds to a 4th-degree polynomial of temperature; green, to a 4th-degree polynomial of temperature plus a 4th-degree polynomial of day-of-year; purple, longitude in addition to the regressors for the green curve; red, surface salinity in addition to the regressors for the purple curve.

and salinity and then from the observed temperature and estimated salinity, and the resulting rms differences at each pressure level are shown. Due to the greater variability in this region, estimates of potential density, like those of salinity, are less accurate than their counterparts for the Gulf of Mexico (Thacker, 2006-this issue). Nevertheless, they should still be useful for correcting a numerical ocean circulation model's density when XBT data are being assimilated.

4. Southeastern sub-region

As the plots of Fig. 5 indicate differences in the TS relationship for the two sub-regions, it is interesting to check how well salinity in the southeast can be estimated using a model designed for the northwest. Fig. 13 shows the southeastern performance for three such models. Their coefficients were determined by fitting to the northwestern training data, and the rms errors are

computed over the combined training and verification data from the southeast, as all were independent of the training data from the northwest. The three models that were evaluated for these data were (1), (4), and (5) determined from *all* training profiles from the northwest. Also shown for comparison are the rms errors for the fourth-degree polynomial of temperature scored for the northwestern verification data.¹⁷ Perhaps surprisingly, in the interval from 200 dbar to 450 dbar the data from the southeast were better estimated than those from the models' native region. This result might have been anticipated from the scatter plot for 400 dbar in Fig. 5, which shows the southeastern data to lie within the northwestern data and to have less spread. Except for this pressure interval, all three models had larger errors when estimating southeastern data, just as had been expected when the region was sub-divided. Errors for

¹⁷ The same curve appears in Fig. 7.

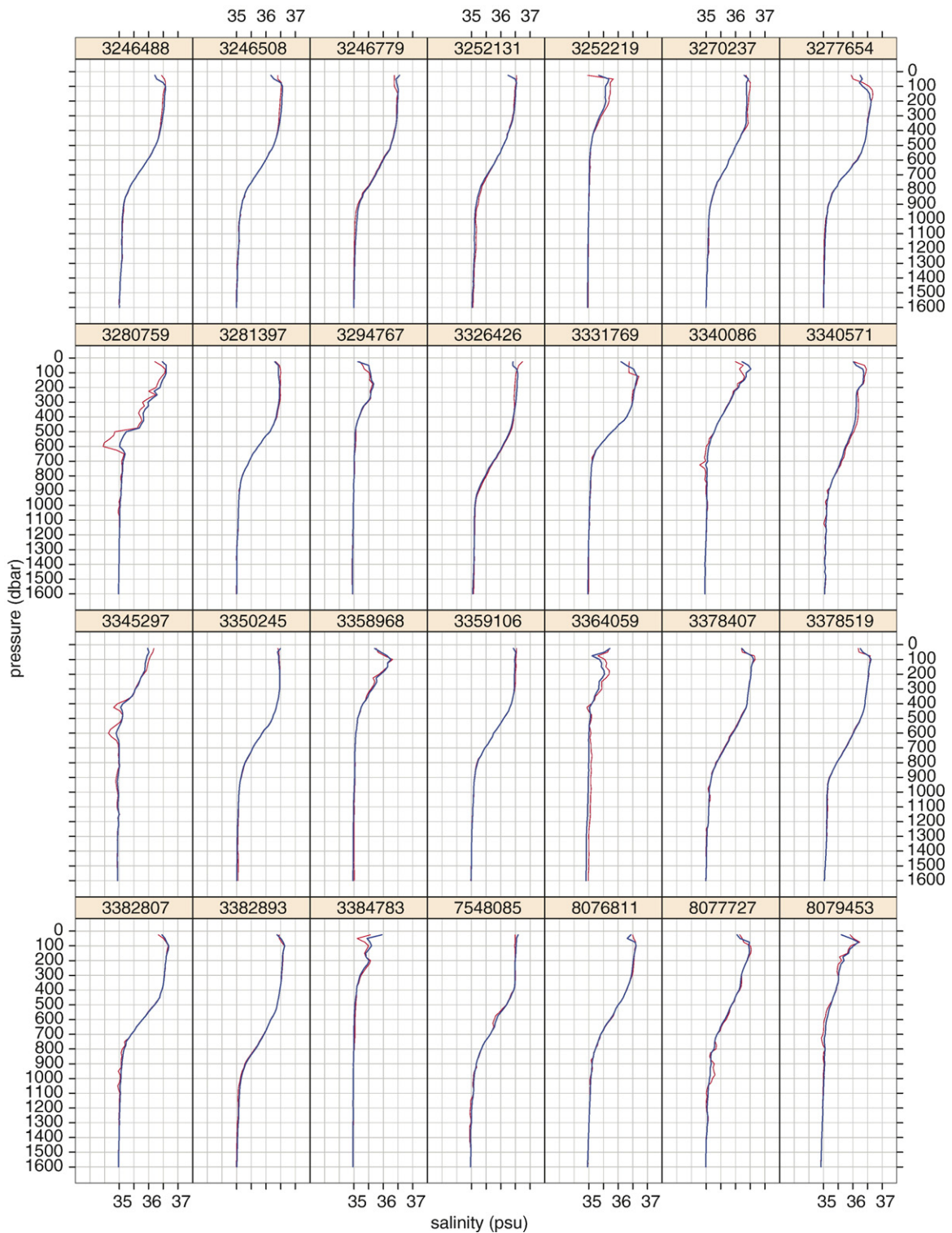


Fig. 11. Comparison of observed (red) and estimated (blue) salinity profiles for 28 randomly selected stations. Estimates were made with $P_4(T) + \tilde{P}_3(d) + \tilde{P}_1(\lambda)$ fitted to the entire set of northwestern training data. Profile identification numbers are indicated on the panel labels.

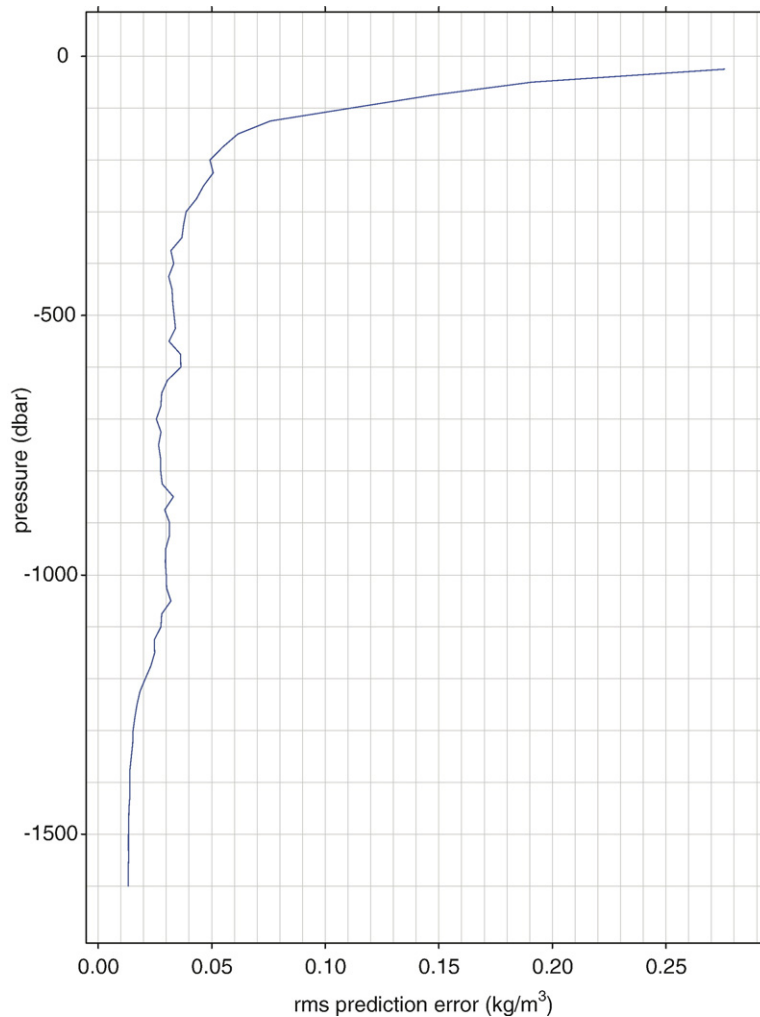


Fig. 12. Root-mean square differences between verification data for potential density and their counterparts estimated using salinity values from $P_4(T) + \tilde{P}_4(d) + \tilde{P}_1(\lambda)$ together with the observed temperatures.

the southeastern data increase beyond 450 dbar until the interval from 950 dbar to 1075 dbar where they are four times larger than those for the northwestern data; they decrease again with further increases in depth but remain at least twice as large as northwestern errors. Fortunately, the large errors for levels deeper than 500 dbar are a problem only for the relatively few long XBT profiles. Models fitted to data in this sub-region should be expected to provide greater accuracy in the upper 200 dbar and below 450 dbar.

Fig. 13 shows that, even with a foreign model, longitude has a beneficial effect for the southeastern data down to 200 dbar, whereas Fig. 10 shows a reduction of rms errors for the native northwestern data only to 100 dbar. This indication of stronger spatial dependence was confirmed when salinity was modelled specifically for the southeastern sub-region. A variety of models were

examined. The absence of the S-shaped TS plots indicated that high-degree polynomials of temperature were not needed, and 2nd-degree proved to be sufficient. Both longitude λ and latitude φ carried information about salinity, but there was no improvement shown when powers of λ or φ were used as regressors. Little additional information was also provided by the day-of-year d .

Fig. 14 shows rms errors for four models:¹⁸ a 2nd-degree polynomial of temperature

$$\hat{S} = P_2(T), \quad (7)$$

¹⁸ Other models were also explored. In particular when (10) was expanded to include unneeded 3rd and 4th powers of T , $\hat{S} = P_4(T) + \tilde{P}_1(\lambda) + \tilde{P}_1(\varphi) + \tilde{P}_1(d)$, overfitting was found to be a problem at some pressure levels with the more parsimonious model giving better results.

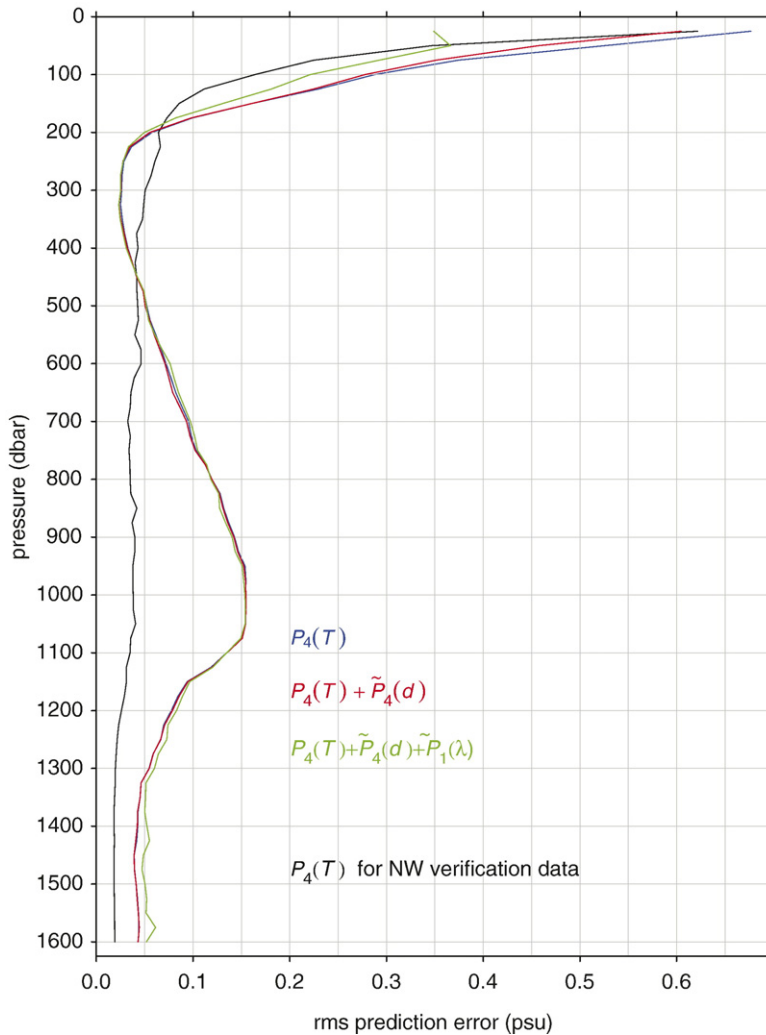


Fig. 13. Root-mean-square differences between data in the southeastern sub-region and their estimated counterparts using models determined by the northwestern training data. Blue curve corresponds to 4th-degree polynomials of temperature; red, to 4th-degree polynomials of temperature and day-of-year; green, to 4th-degree polynomials of temperature and day of year plus longitude. For reference, the black curve indicates the rms errors for the northwestern verification data using 4th-degree polynomials of temperature. (For interpretation of the references to color in this figure legend, the reader is referred to the web version of this article.)

which is expanded to include a term proportional to longitude

$$\hat{S} = P_2(T) + \tilde{P}_1(\lambda), \quad (8)$$

which in turn is expanded to include a term proportional to latitude

$$\hat{S} = P_2(T) + \tilde{P}_1(\lambda) + \tilde{P}_1(\phi), \quad (9)$$

and once more to include a term proportional to day-of-year

$$\hat{S} = P_2(T) + \tilde{P}_1(\lambda) + \tilde{P}_1(\phi) + \tilde{P}_1(d). \quad (10)$$

These models were fitted to the 114 southeastern training profiles and the rms errors reflect their ability to

reproduce the salinity of the remaining 114 southeastern profiles, which were set aside for independent verification. At all levels these errors are considerably smaller than those shown in Fig. 13 for the northwestern models scored against the southeastern data.

Using models native to the subregion, estimates of near-surface salinity are much more accurate for the southeastern sub-region than for the northwestern. Near the surface temperature provides more information about salinity for this sub-region than it did in the northwest, but longitude was less help. However, longitude provided more information about salinity at depth than it did in the northwest. While latitude was not useful in the northwest, here it is responsible for much of this improved near-surface skill,

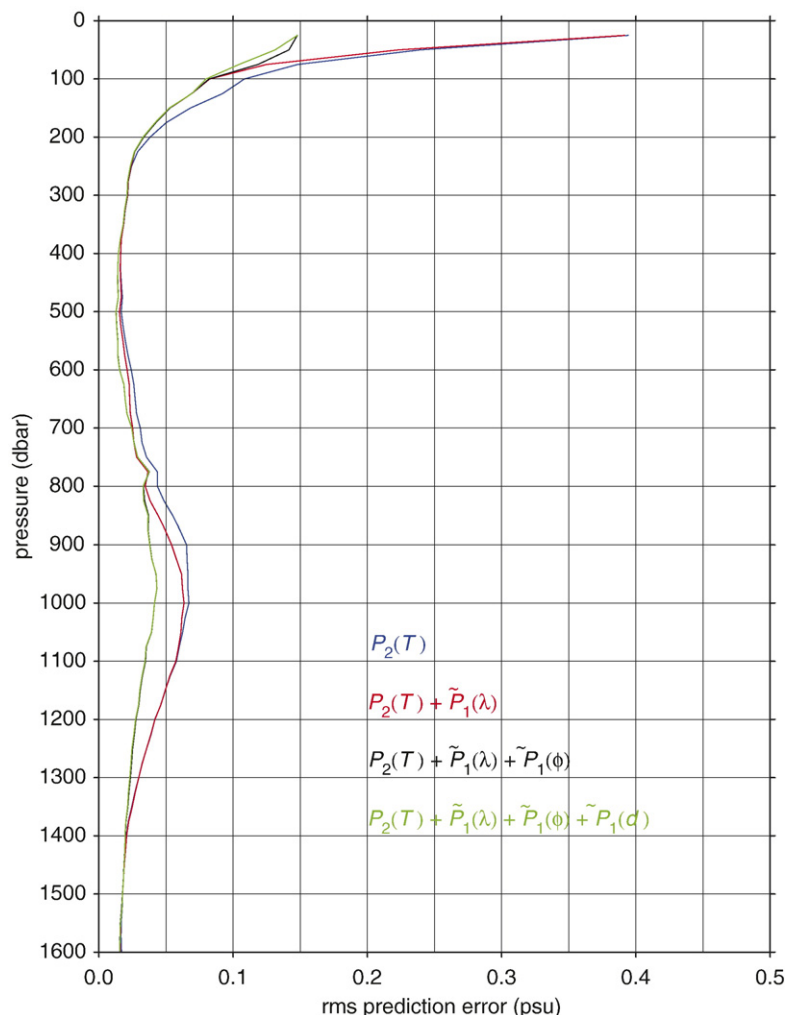


Fig. 14. Root-mean-square differences between verification data in the southeastern sub-region and their estimated counterparts using models determined by the southeastern training data. Blue curve corresponds to 2nd-degree polynomials of temperature; red, to 2nd-degree polynomial of temperature plus longitude; black, to 2nd-degree polynomial of temperature plus longitude and latitude; green, to 2nd-degree polynomial of temperature plus longitude, latitude, and day-of-year. (For interpretation of the references to color in this figure legend, the reader is referred to the web version of this article.)

and it substantially increases skill for the deeper levels. The error maximum around 1000 dbar is similar to that seen in Fig. 13, but with these models it is much smaller; latitude, especially, and also longitude are responsible for increased skill in the interval from 500 dbar to 1400 dbar centring on the error maximum. Including day of the year as an additional regressor (model 10) gave noticeable improvement only at 50 dbar and 75 dbar, as the green curve was essentially the same as the black everywhere else, and polynomials of d did no better, perhaps because the sampling provided by the training data did not capture the seasonal cycle. More generally, salinity can be estimated more accurately in the southeastern sub-region than in the northwestern where variability is greater. In the important

interval from 400 dbar to 600 dbar, rms errors are seen to be half as large as those shown in Fig. 7 for the northwestern sub-region.

5. Performance at the boundary between sub-regions

While the question of how to partition the region into a southeastern Sargasso Sea region and a northwestern Gulf Stream region certainly deserves more attention, the question of continuity of estimates from one sub-region to the next is also important. To examine this issue salinity profiles for stations close to the arbitrary partition line of Fig. 2 were estimated using models from either side of the partition. The boundary stations were the verification

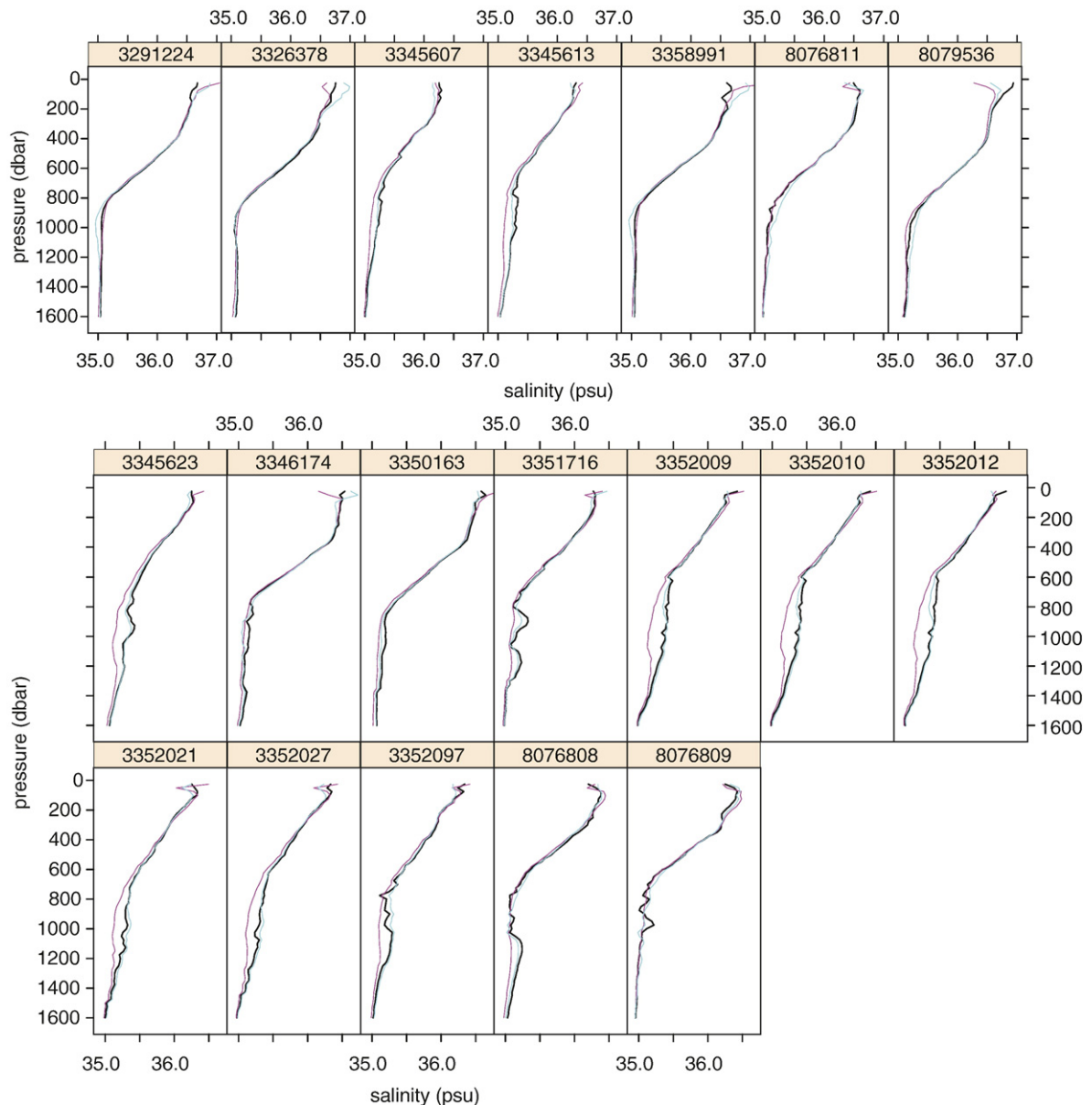


Fig. 15. Estimates for border stations in northwestern (upper 7 panels) and in southeastern (lower 12 panels) sub-regions. Black, observed; magenta, NW model (Eq. (5)); cyan, SE model (Eq. (10)). (For interpretation of the references to color in this figure legend, the reader is referred to the web version of this article.)

stations within the band swept out by sliding the partition line 1° north (7 stations) and 1° south (12 stations), and the models were those that performed best in each region, i.e., Eq. (5) fitted to the northwestern training data and Eq. (10) fitted to the southeastern training data. The results are shown in Fig. 15.

The seven profiles in the top row of panels of Fig. 15 are from the northwestern side of the partition line. For three, namely profiles 3291224, 8076811, and 8079536, the northwestern model (magenta curves) more closely ap-

proximates the observed salinity (black curves), while the southeastern model (cyan curves) approximates the other four profiles better. For most of the twelve profiles from the southeastern side of the partition the southeastern model clearly outperforms the northwestern, for a few their performance is similar, but there is no case where the northwestern model is clearly best. For both sets of profiles the differences are generally largest for the pressure range corresponding to the error maxima of Figs. 13 and 14 where latitude gives an advantage to the southeastern

model. The southeastern model's better performance in this boundary zone suggests that the partition should be moved north and/or east. However, the partition need not be a straight line and might be different at different depths.

As the salinity estimates are intended for assimilation into numerical models, the possibility of introducing spurious density gradients in the vicinity of artificial regional boundaries is a concern. If the boundaries are chosen so that the models from opposite sides have similar skill in the vicinity of the boundary, then averaging the estimates might insure continuity. For example, at the boundary the estimates can be equally weighted, with weights shifting in favour of the region's native model with distance from the boundary.

6. Conclusion

For the purposes of estimating salinity profiles to complement XBT data, the 30° longitude by 20° latitude study region, after excluding the continental shelf, should be divided into two sub-regions: a northwestern sub-region that is more closely associated with the Gulf Stream and its recirculation and a southeastern sub-region that is more characteristic of the central North Atlantic. The co-variability of salinity with temperature differs in the two sub-regions especially in the upper 200 m and below 500 m, as does its co-variability with longitude, latitude, and day-of-year. Consequently, different empirical models are needed for each sub-region. The partition of the region, like the location of the rectangle, was arbitrary and exploratory, and the question of determining optimal regions for salinity estimation certainly deserves more attention. Still, the variability within each of the two sub-regions is sufficiently homogeneous that salinity can be estimated with reasonable accuracy.

Within each sub-region salinity was modelled independently at 64 different levels ranging from 25 dbar to 1600 dbar, spaced at 25 dbar intervals. While the best model at one pressure level is not necessarily the best at another, the problem of overfitting is not serious and the best models for each region could be used at all levels. Nevertheless, it is not wise to seek a model with many terms that might be appropriate in all regions. Adding two unneeded powers of temperature to the best model for the southeastern sub-region gave noticeably worse results for some levels, and similar problems can be expected whenever the principal of parsimony is violated.

For the northwestern sub-region 4th-degree polynomials of temperature were found to work well at all levels, while 3rd-degree polynomials did not perform significantly worse and at some levels straight lines or

parabolas were sufficient. For most levels there was no need to account for time of year or for the position within the sub-region where the estimate was needed; near the surface, however, this was not the case. In the upper 100 dbar where temperature provides relatively little information about salinity, using the first four powers of day-of-year as additional predictors was able to reduce the rms estimation error by about 25%. In the upper 50 dbar, longitude provided an additional reduction of about the same amount. If surface salinity were available, it too would give another additional error reduction of this magnitude, with the cumulative effect bringing the error at 25 dbar from about 0.58 psu to 0.30 psu. The accuracy for deeper levels is much better with rms errors decreasing from about 0.05 psu at 300 dbar to 0.02 psu at 1600 dbar.

Two alternative methods for estimating salinity were examined for the northwestern sub-region and were found to be inferior. The first, which approximates salinity by its climatological mean on pressure surfaces, is attractive because it can be easily implemented using published climatologies. Unfortunately, its failure to exploit the strong TS co-variability cause it to have much larger errors; its rms errors at 400 dbar are more than an order of magnitude larger than those for the regression model and at 1600 dbar, double. The second approximates salinity by its climatological mean on temperature surfaces; as such means can be approximated using data for the climatological mean profiles, it also offers the possibility of easy implementation. While better than the first alternative, this method also had larger errors than the regression models, roughly double for all depths.

While the models fitted to the northwestern data provided quite good estimates for the southeastern sub-region in the interval between 200 dbar and 450 dbar, better in fact than they provided for the northwestern sub-region, their performance was poor at other levels, so native southeastern models were needed. In the southeastern sub-region a 2nd-degree polynomial of temperature served well at all depths and the unneeded higher powers used in the northwest proved to be a liability. Another remarkable result was that here more information was provided by the location of the station than was the case for the northwestern sub-region. Longitude proved useful from the surface to 300 dbar and again from 550 dbar to 1050 dbar; and latitude, which was not helpful in the northwest, provided even more information from the surface to 100 dbar and again from 350 dbar to 1350 dbar. Day-of-year was less useful than in the northwest, but this may be an artificial result of the sample of stations that were used. In both regions the seasonal cycle for the upper levels deserves a more careful treatment.

The case in Fig. 11 (profile 3364059) with a systematic difference between estimated and measured salinity over a wide range of pressures is remarkable because it can be interpreted as a problem with that profile's calibration. It should not be difficult to search the CTD archives for similar deep offsets using cruise information to check whether this interpretation is correct. If it is, a profile's mean offset at depth could be used to correct its miscalibrated salinity data.

The major conclusions are (1) that salinity can be accurately estimated in the vicinity of the Gulf Stream and (2) that estimates improve if the region of the Gulf Stream is separated from that of the Sargasso Sea. The question of how best to set regional boundaries remains, as does the related question of how to guarantee continuity of estimates at regional boundaries. As the project progresses and more regions are examined, these question should be answered.

Acknowledgements

This work was supported by the National Oceanographic Partnership Program and by the Atlantic Oceanographic and Meteorological Laboratory.

References

- Armi, L., Bray, N.A., 1982. A standard analytic curve for potential temperature versus salinity for the Western North Atlantic. *Journal of Physical Oceanography* 12, 384–387.
- Conkright, M., Locarnini, R.A., Garcia, H.E., O'Brien, T., Boyer, T., Stephens, C., Antonov, J., 2002a. World Ocean Atlas 2001: Objective Analysis, Data Statistics, and Figures, CD-ROM Documentation. National Oceanographic Data Center Internal Report, vol. 17. NOAA.
- Conkright, M., O'Brien, T.D., Boyer, T., Stephens, C., Locarnini, R.A., Garcia, H.E., Murphy, P.P., Johnson, D., Baranova, O., Antonov, J.I., Tatusko, R., Gelfeld, R., 2002b. World Ocean Database 2001. National Oceanographic Data Center Internal Report, vol. 16. NOAA. CD-ROM Data Set Documentation.
- Fofonoff, N.P., 1977. Computation of potential temperature of seawater for an arbitrary reference pressure. *Deep-Sea Research* 24, 489–491.
- Iselin, C.O., 1936. A study of the circulation of the western North Atlantic. *Papers in Physical Oceanography and Meteorology* 4 (4), 3–101.
- Loder, J.W., Petrie, B., Gawarkiewicz, G., 1998. The coastal ocean off north-eastern North America: a large-scale view. *The Sea*, vol. 11. John Wiley and Sons, pp. 105–133. Ch. 5.
- Millero, F.J., Poisson, A., 1981. International one-atmosphere equation of state of seawater. *Deep-Sea Research* 28A, 625–629.
- R Development Core Team, 2004. R: A language and environment for statistical computing. R Foundation for Statistical Computing, Vienna, Austria, ISBN 3-900051-00-3. <http://www.R-project.org>.
- Richardson, P.L., 1983. Gulf Stream rings. *Eddies in Marine Science*. Springer-Verlag, pp. 19–45. Ch. 6.
- Stommel, H., 1947. Note on the use of the T–S correlation for dynamic height anomaly calculations. *Journal of Marine Research* 85–92.
- Thacker, W.C., 2006-this issue. Estimating salinity to complement observed temperature: 1. Gulf of Mexico. *Journal of Marine Systems*. doi:10.1016/j.jmarsys.2005.06.008.
- Thacker, W.C., Lee, S.-K., Halliwell Jr., G.R., 2004. Assimilating 20 years of Atlantic XBT data into HYCOM: a first look. *Ocean Modelling* 7, 183–210.
- Tomczak, M., Godfrey, J.S., 2003. *Regional Oceanography: An Introduction*. Daya Publishing House, Delhi.
- Venables, W.N., Ripley, B.D., 2002. *Modern Applied Statistics with S-Plus*. Springer-Verlag, New York.
- Watts, D.R., 1983. Gulf Stream variability. *Eddies in Marine Science*. Springer-Verlag, pp. 114–144. Ch. 6.
- Wong, A.P.S., Johnson, G.C., Owens, W.B., 2003. Delay-mode calibration of autonomous CTD profiling float salinity data by θ -S climatology. *Journal of Atmospheric and Oceanic Technology* 20, 308–318.
- Worthington, L.V., Metcalf, W.G., 1961. The relationship between potential temperature and salinity in deep Atlantic water. *Rapports et Procès-Verbaux des Réunions* 149, 122–128.